SMALL IMPACT CRATER CLUSTERS IN HIGH RESOLUTION HIRISE IMAGES. B. A. Ivanov[1], H. J. Melosh[2], A. S. McEwen[2], and the HiRISE team, [1]Institute for Dynamics of Geospheres, RAS, 119334, Moscow, Russia, baivanov@idg.chph.ras.ru, [2]University of Arizona, Department of Planetary Sciences, Tucson, AZ, 85721.

Introduction: Impact crater clusters or crater strewn fields from primary impacts are well known for planets with atmospheres such as Earth and Venus. Observations [1] and theoretical analysis prove that the cause of crater clustering is atmospheric breakup of meteoroids [2-5]. The presence of impact crater clusters on Mars has been revealed by MOC images [6, 7]. Due to the small density of the atmosphere on Mars, the size of clusters controlled by lateral motion of fragments is about 10 to 100 meters. The HiRISE image scale of 0.25-0.32 meters per pixel allows us for the first time to resolve details of small crater fields on Mars.

New Craters on Mars: Repetitive imaging of Mars by various spacecraft revealed 20 potential "new" impact sites [8]: impact craters with documented time periods of formation, assuming that the appearances of dark spots correspond to crater formation. HiRISE was targeted at the same sites and confirmed 19 of Malin's "new" craters as fresh impact craters, although whether or not they formed in the past decade remains unclear [9]. We compare measurements published in [8] with HiRISE data. Impact site numbers are designated as M1 to M20 after [8].

Crater type.. Of the total confirmed 19 very recent impact sites we see a single crater (4 cases) or a single major crater with much smaller companions (2 cases, 3 to 9 visible companion craters). Tentatively we name these impact sites as Type 0. In 6 cases a major (largest) crater has many companion craters (from 5 to 60 detected craters) – the situation tentatively classified as Type 1. In 5 cases the cluster includes many craters (from 12 to 70 detected) with or without one major crater. Taking into account the size-frequency distribution (SFD) described below (Fig. 1) we labeled these as Type 2. In two cases (PSP 003172_1870=M20 and PSP 005942_1825=M8) crater fields are denseley populated (>2000 and >400 detected craters, repectively). Tentatively we labeled these two sites as Type 3.

In summary, a single crater or one major crater formed in ~65% of impacts (12 of 19 cases). Prominent multiple clusters (5 of 19) and "overpopulated" clusters (2 of 19) account for ~35 % (7 of 19). Although many of these new primary craters produced radial chains of relatively distant secondary craters, the tight clusters considered here are not consistent with typical secondary craters.

Crater size and cratering rate. The accuracy of single crater measurements in HiRISE images with ImageJ software, even with 0.25 m pixels, is limited by image signal:noise ratio, the optical point-spread function, illumination geometry, target background roughness, and crater shape deviation form a simple circle or ellipse. Direct comparison of crater diameters in simple situations (6 cases of our Type 0) give an average D_{HiRISE}/D_{MOC} ratio of 0.96 (ranging from 0.89 to 1.05).

The number of small craters detectable in HiRISE images is much greater than from MOC.

To compare absolute fluxes on the Moon and Mars it is important to estimate the effective size of craters on a hypothetical airless Mars. Without quantitative constraints on target properties we assume that the best first-order approximation is that D is proportional to D_P (D is the crater diameter, D_P is the projectile diameter). However, target materials appear to vary from thick dust mantles to coherent bedrock (with a very thin dust cover). With better constraints on target strength properties we would need to reconsider some numerical characteristics listed below. We measured the diameters of all detected craters in each cluster and use the value of $D_{eff}=(\Sigma D_i^3)^{1/3}$ as a simple measure of an effective crater that would be created on an atmosphereless Mars. With the much larger number of measured small craters our D_{eff} in several cases is 1.5 to 1.7 times larger than in [8]. With a standard $2^{0.5}$ binning of craters used to present the crater SFD the number of craters is changed only in a couple of bins (using D_{eff} for a would-be single crater). We interpret the largest diameter bins as complete, whereas the number of craters falls off sharply at smaller diameters due to image detection limits. Formally the number of craters for a given area measured in ~7 years corresponds to Hartmann's [9] 4-year old model surface. Uneven distribution of recognized craters in the nominal area [11] and/or revised (older) ages for the actual impact events would increase the modeled age.

Effective diameters of "new" impact craters listed in [8] range from 10 to 33 m, while the smallest detected craters are 0.75 to 1m.

Size of Clusters: The rarefied atmosphere of Mars even near the surface corresponds to ~30 km of altitude in the terrestrial atmosphere. The Passey&Melosh model (PM80, [2]) of atmospheric breakup gives the maximum separation of fragments on the surface for breakup at H*~22 km above the surface of Mars.

~75% of the maximum separation will be observed for fragmentation at altitudes from ~38 km to ~10 km. At these altitudes the stagnation pressure for average asteroid-type orbit (entry velocity of 10 kms^{-1}) is in the range of ~0.5 to ~5 bar. Fragmentation of meteoroids in the terrestrial atmosphere is well known (e.g. [12]).

PM80 [2] with separation coefficients from 3D numerical simulations [3] gives the maximum separation of two fragments at the surface of ~12 m for a vertical impact of meteoroids with density of 3 gcm^{-3}. Hence for vertical impacts the separation is comparable to the smallest observed effective crater diameter (10 m). The maximum separation along the trajectory increases for small incidence angles α proportional to $(\sin \alpha)^{-1}$ remaining the same in the lateral direction.

We measured separation distances of crater centers relative to the major crater (if exists) or to the center of gravity of the fragment swarm (assuming that the fragment masses are proportional to D^3). The spatial distribution of craters on surface is used to estimate possible range of trajectory inclinations. Crater positions are projected to the plane perpendicular to the trajectory (PPT); in the PPT plain the cross-sections of a meteoroid's fragment cone should be circles with radii determined by the initial lateral velocity of fragments at the breakup point and the flight time after breakup. We use a simple average, $<r>$, and D^3– weighted values, r_w, to quantify the width of a fragment swarm in the PPT plane. Individual distances, r_i, are measured from the center of the dominant major crater (if exists) and/or from the effective "center of gravity" of the crater field in the PPT plane.

We estimated the maximum density of a meteoroid (ρ_m) and minimum breakup height (H^*) admissible for the isolated fragmentation events with the PM80 model (small chips separation from the main meteoroid body) and for a newly developed cascade fragmentation model where individual fragmentation events are described with the PM80 model. All available data are reduced to a parameter that expresses the separation of two equal fragments after breakup at a nominal vertical impact, r_{eq90}. The value of r_{eq90} depends on the assumed density and breakup altitude.

For Type 0 clusters (single crater or one major dominating crater) in 3 of 4 cases the solution assumes ρ_m ~3 g cm^{-3} and H^*~ 8 to 18 km (close to ordinary chondrites [10]). In one case (M5=PSP_004038) only ρ_m ~0.5 g cm^{-3} and H^*~ 22 (altitude of maximum separation) explain the cluster width in the PM80 model. For Type 1 clusters analysis gives an apparent meteoroid density of 1.8 to 3 g cm^{-3} in 4 of 5 cases. The 5th Type 1 cluster solution (M16=PSP_003527) results in an apparent density of 1.5 g cm^{-3}. Four Type 2 cluster solutions show an apparent density in the range of 1.8 to 3 g cm^{-3}. Both Type 3 shower solutions converge if one assumes a density of about 1 g cm^{-3}.

Conclusion: Simple modeling of 15 dated cluster-forming cratering events on Mars [8] shows that in 11 cases the observed cluster dispersion may be explained with simple models (PM80 and a new cascade model which will be presented at the conference) using an efficiency of lateral fragment acceleration proposed in [3] and assuming densities in the range 1.8 to 3 gcm^{-3}. Together with 4 single craters these clusters give ~80% of dated impacts (15 of 19). In 4 cases the observed cluster dispersion requires a small meteoroid density (0.5 to 1.5 gcm^{-3}). However, such a low density should be accompanied by a high ablation coefficient [12]. These low-density cases require further analysis with more sophisticated models.

References: [1] Melosh (1989) Impact Cratering. [2] Passey Q. R. and H. J. Melosh (1980) *Icarus, 42,* 211-233. [3] Artemieva N. A. and V. V. Shuvalov. (2001) *JGRE, 106,* 3297-3310. [4] Korycansky D G. and K. J. Zahnle (2004) *Icarus, 169,* 287-299. [5] Korycansky D G. and K. J. Zahnle (2005) *PSS, 53,* 695-710. [6] Popova O. P. et al. (2003) *MAPS 38*, 905-925. [7] Popova O. P. et al. (2007) *Icarus 190*, 50-73. [8] Malin M.C. et al. (2006) *Science, 314*, 1573-1577 [9] McEwen A.S. et al., LPSC 2007. [10] Hartmann W.K. (2005) *Icarus 174*, 294-320. [11] Kreslavsky M. A. (2007) *7th Int. Conf. on Mars*, #3325. [12] Cepleha Z. et al. (1998) *Space Sci. Rev. 84*, 327-471.

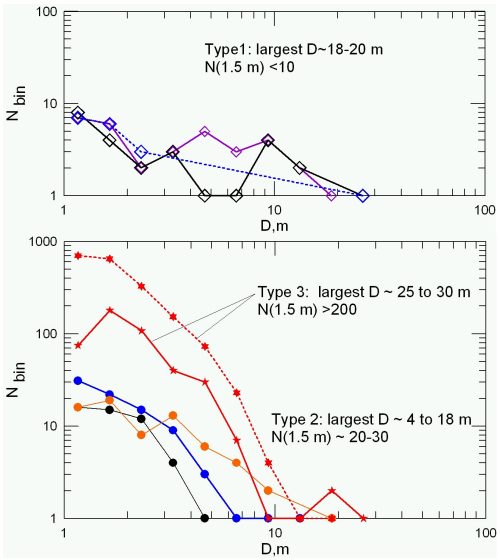

Fig. 1. Size-frequency distributions of craters in clusters illustrating the variability of the fragmentation style of meteoroids in Martian atmosphere. Tentatively we assume that in Type 1 events small fragments mostly spall off the main body while in Type 2 and 3 events the small size "tail" of fragments forms in a cascade of fragmentation events.